ICIC Express Letters
Volume **16**, Number **10**, October **2022**

pp. 1101–1109

DESIGN AND PERFORMANCE ANALYSIS OF THREE PHASE SENSORLESS BLDC MOTOR FOR UNMANNED AERIAL VEHICLE APPLICATION

Heri Suryoatmojo, Ilham Reindyto, Mochamad Ashari
Feby Agung Pamuji and Ronny Mardiyanto

Department of Electrical Engineering
Institut Teknologi Sepuluh Nopember
Kampus ITS, Sukolilo, Surabaya 60111, Indonesia
{ suryomgt; ashari; feby }@ee.its.ac.id; reindyto.17071@mhs.its.ac.id; ronny@elect-eng.its.ac.id

Received September 2021; accepted December 2021

Abstract. *The advantages of Brushless DC (BLDC) motors are high efficiency, capable of operating at high speeds, easy maintenance, and high torque. Core material and stator winding are important things to consider in designing of this motor. The stator core is generally made of silicon steel with a material thickness of about 0.1 mm. However, this material is not easy to find in the Indonesian market. Therefore, this research presents the design process of a BLDC motor prototype using materials available in the Indonesian market. The simulation uses Finite Element Analysis (FEA) method to determine the electromagnetic parameters of the model. Meanwhile, the prototyping process is done manually by utilizing the original rotor and its frame. Due to the small size of the motor, torque measurements are made using a lab made torque meter. Testing is done by comparing the performance of the prototype with the original motor. The efficiency parameter obtained from the prototype is 13.57% of the efficiency of the original motor.*
Keywords: BLDC, Prototype, Reverse engineering, Torque meter design

1. **Introduction.** The development of Unmanned Aerial Vehicle (UAV) cannot be separated from development of propulsion which provides thrust to the vehicle [1]. UAVs with engine propulsion always have weight problems because they have to carry liquid fuel. In recent decades, UAVs have been demanded to be lighter, more agile, and easier to operate so that they can be applied to a wider use. Of all types of UAV propulsion, Brushless DC motors are always considered because they have the characteristics of light weight, durable, simple, and can be operated at high speeds so that they are in line with today's demands [1,2].

Brushless DC motor does not require a brush so it is easy to maintain and efficient in use. There are various designs for different applications. In designing a BLDC motor for UAV efficiency, size, and weight are crucial aspect [3]. In addition, several parameters that need to be considered in designing a BLDC motor are magnetic properties of material used, air gap, dimensions of the motor, and several other parameters that can optimize the BLDC motor [4]. From the existing design parameters, material is a parameter that mostly determines performance of BLDC motor, because apart from carrying magnetic properties, the material also determines weight, size, and durability of the design [5-10].

Several studies related with BLDC motors are usually limited to controlling and modeling of this motor. In [2,14], this research only focuses on simulation and control of BLDC motor. [3,4] propose BLDC motor design for UAV application. However, all materials used in design and simulation are mostly not available domestically. Therefore, this paper

DOI: 10.24507/icicel.16.10.1101

proposes the design and the performance analysis of BLDC motors made using materials available domestically.

The method to realize this prototype is started by observing the existing T-Motor AT3520 for the reference. After all parameters related with the physics and geometry of this motor are obtained, then, perform modelling the BLDC motor based on the obtained parameters by using software application. The important step of this research is prototyping of this motor by using the material available in Indonesia. Finally, investigate the performance of this motor by comparing with the reference motor.

2. **BLDC Motor Modelling.** BLDC motor, also known as permanent magnet synchronous motor, requires an Alternating Current (AC) as an input for this motor. In order to generate AC voltage, an inverter system is required to convert DC voltage into three-phase AC voltage with a phase difference of 120°. If one phase is taken, the equivalent circuit of a BLDC motor is obtained as shown in Figure 1 [2].

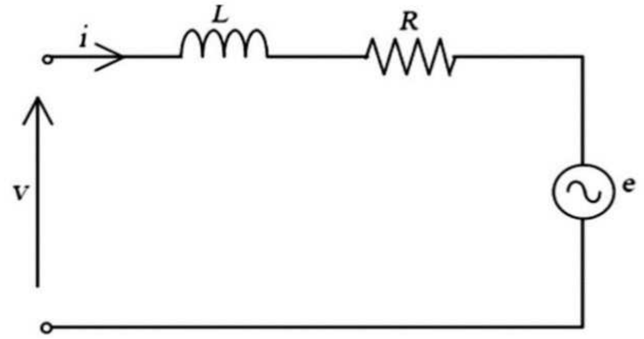

FIGURE 1. BLDC motor equivalent circuit

This circuit is a winding on the stator. From the circuit there is a voltage source (v) which in the unmanned aerial vehicle is a LiPo battery. There is a current (i) flowing in phase through the inductor (L) and resistor (R). The two components represent inductance of coil and resistance of the conductor. A BLDC motor has a back-Electromotive Force (back-EMF) (e) with the opposite voltage from the source. Back-EMF arises due to magnetic induction that rotates against the stator winding so that it affects the voltage that enters the DC brushless motor. From the circuit we get formula [7]

$$V = Ri + L\frac{di}{dt} + e \tag{1}$$

where V is voltage, R is resistance, L is inductance and e is back-EMF. The output of a BLDC motor is mechanical energy in the form of torque. The equation that represents the torque on the BLDC motor conductor is as follows [13]:

$$\tau_c = BI_cL_cR_{si} \tag{2}$$

where τ_c is torque, B is flux density, I_c is current through conductor, L_c is active length of the motor in mm and R_{si} is stator inner radius in mm. Speed controller has a three-phase inverter with a difference of 120° so that 2 phases will be powered at a certain time. So, the total torque generated is [13]

$$\tau = 2 \times 2pBI_cn_sL_cR_{si} \tag{3}$$

Here τ is torque, p is number of pole pairs, n_s is number of turns in a slot. The power output is generated [13].

$$P_m = \tau \cdot \omega \tag{4}$$

where P_m is mechanical power and ω is angular speed in rad/s. Copper losses are the most dominant losses in BLDC motors [8]. This loss is due to the resistive nature of the enameled copper wire used as conductor. Symbolized by P_{cu}, these losses are defined in the formula [13].

$$P_{cu} = 2R_{ph}I_s^2 \tag{5}$$

where P_{cu} is stator copper loss, R_{ph} is phase resistance, I_s is current from DC source. While R_{ph} and I^2 are the winding phase resistance and the rms value of the motor phase current. In addition, there is an iron core loss caused by the electromagnetic characteristics of the stator core material. To calculate it, we need a constant set by the material manufacturer [10].

$$P_{fe} = k_h f \hat{B}^{\alpha} + \frac{k_e}{2\pi^2}\left\{\frac{dB}{dt}\right\}_{rms}^2 \tag{6}$$

where P_{fe} is stator core loss, k_h, k_e are material constant and f is the frequency of system.

3. Design, Simulation, and Prototyping.

3.1. **Stator construction.** Research begins by observing the technical specification and electrical characteristic of the reference motor [11]. Here, all data from this motor are then analyzed by FEA software application in order to know detailed characteristic motor such as speed, current, power consumption and the thrust of motor. Then, measure the dimension of the stator, rotor and diameter of the copper wire of the winding as seen in Table 1. For designing the protype of BLDC motor, this study considers the materials of core and copper wire based on materials available in Indonesia. Here, carbon steel metal is selected because it is very easy to find and has better electromagnetic properties.

Table 1. Motor parameter

Parameter	**AT3520**	**Prototype**
Pole number	14	14
Slot number	12	12
Magnet material	Neodymium	Neodymium
Rotor material	M800-100A	M800-100A
Stator material	Silicon Steel 0.1 mm	Carbon Steel (Fe.C) 1 mm
Shaft material	304 Stainless Steel	304 Stainless Steel
Conductor	Copper: 5.77e7 Ω^{-1}/m	Enameled wire 1.37 Ω/m
Wire diameter	0.2 mm	0.2 mm
Stator diameter	35 mm	35 mm
Slot depth	8.05 mm	8.25 mm
Slot opening width	1.5 mm	1.3 mm
Tooth tip thickness	1.5 mm	1.5 mm
Tooth width	2.48 mm	2.38 mm
Turns	5	5
Strand in Hands	27	27

For conductors, it is obtained that the reference motor uses copper wires with a diameter of 0.2 mm which is equivalent to the American Wire Gauge (AWG) 32 standard. Meanwhile, rotor part is still considering to use the same material as T-Motor AT3520 frame. The winding type used is in delta connection with lap configuration. The design of stator geometry of the proposed prototype is modified based on the electrical calculation and can be seen in Figure 2.

In BLDC motor stator, there is a coil wrapped around the stator slot as seen in Figure 2. The coils are wound using a delta configuration with the lap winding method. It uses 54 parallelly stranded conductor with the diameter as 0.2 mm per phase. Then, this

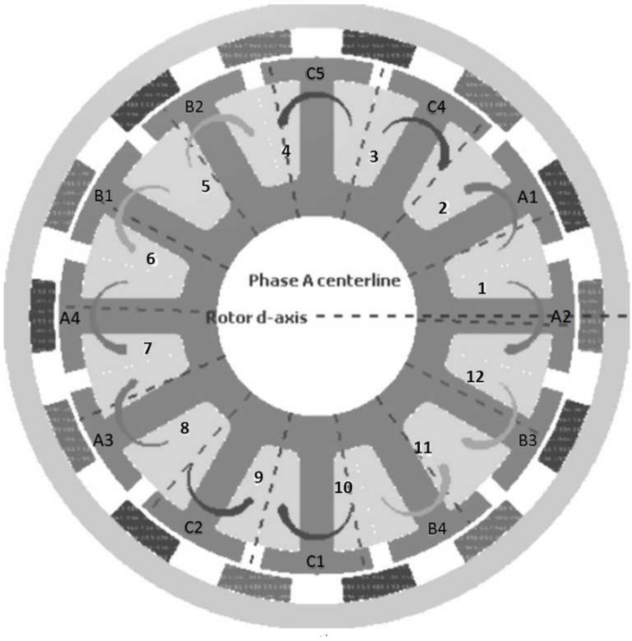

Figure 2. Stator and winding construction

Table 2. Winding step in the stator of BLDC motor

Phase	Winding	Go	Return	Turns
Phase A	1	1	2	5
	2	1	12	5
	3	8	7	5
	4	6	7	5
Phase B	1	5	6	5
	2	5	4	5
	3	12	11	5
	4	10	11	5
Phase C	1	10	9	5
	2	8	9	5
	3	3	4	5
	4	3	2	5

winding is divided into two different polarities. To form the winding in phase A, 27 parallel conductors are wounded on tooth of A1 through slot 1 and then back through slot 2 to form a counterclockwise winding if the point of view is from the outside of the stator. The winding process is carried out 5 turn. Followed by winding on tooth A2 through slot 1 then back through slot 12 to form a clockwise loop. The process is continued by winding tooth 8 on with counter clockwise direction. A counterclockwise winding on tooth 7 is the end of phase A. All these steps are explained and shown in Table 2.

3.2. **Torque and power calculation.** UAVs require a large torque to weight ratio. This is because the UAV propeller has a length of up to 5 times the outer diameter of the motor. In this section, it will be explained about the calculation of the maximum torque of the motor design. The formula to find maximum torque ($\tau_{\max}$) of BLDC motor is as follows:

$$\tau_{\max} = 2 \times 2pBI_c n_s L_c R_{si}$$
$$\tau_{\max} = 2 \times 2 \times 14 \times 1.45 \times 14.31 \times 5 \times 0.0206 \times 0.0175$$
$$\tau_{\max} = 2.0944 \text{ N·m} \quad (7)$$

Here the design has $p = 14$ poles, the maximum flux density (B) of the material is 1.45 Tesla, with the maximum current passing through 27 parallel conductors of AWG 32 (I_c) as 14.31 A. Then the number of turns of the winding (n_s) is 5 turns, the length of the conductor in the magnetic field (L_c) is 0.0206 m and the stator radius (R_{si}) is 0.0175 m.

For the calculation of the maximum output power P_m on the motor using the following formula:

$$P_m = \tau_{\max} \cdot \omega$$
$$P_m = 2.0944 \times 387.6725$$
$$P_m = 811.94 \text{ W} \tag{8}$$

where the ω is angular velocity in rad/s. This design delivers an output power of 62.45% of the original rated power.

3.3. **Performance of the prototype under FEA analysis.** After determining and designing the construction of the stator, the next step is performing the characteristic of the proposed BLDC motor. Simulation using FEA software is utilized to obtain the average torque, torque vs speed characteristics. The inputs for FEA software are voltage, dimension of the motor, configuration of the winding, rated current and rated speed of the BLDC motor. Figure 3 shows the average torque vs speed characteristic of the BLDC motor. It shows that torque is inversely proportional to the speed.

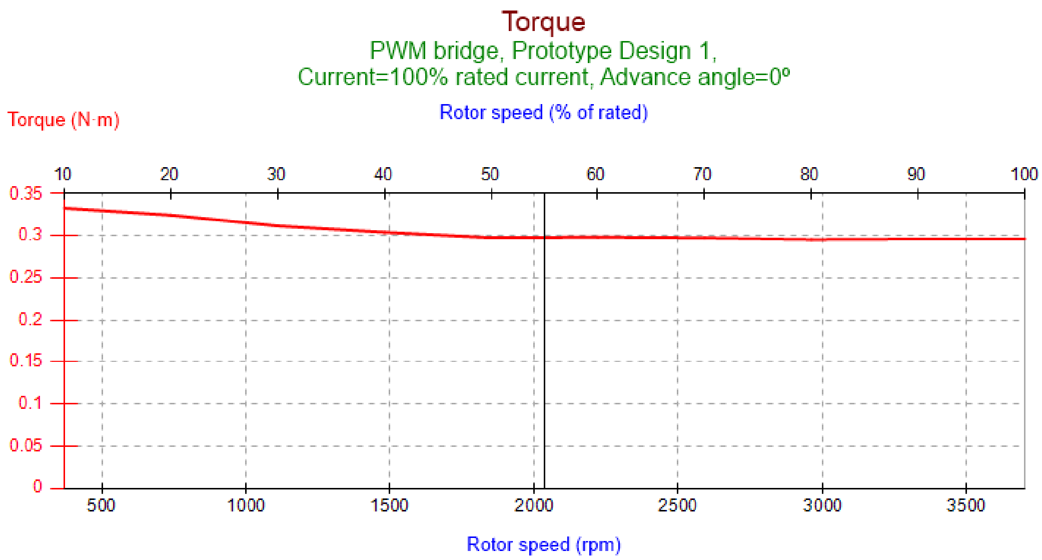

FIGURE 3. Torque vs speed simulation

3.4. **Prototyping process.** The first step of prototyping process is by printing material using laser cutting method. Cutting process is precise enough to produce the desired stator lamination shape. After cutting process, sheet metal is rubbed on size 220 abrasive paper to flatten metal surface. Then arrange piece of stator sheet into a laminate to form the stator core. In order to strengthen the lamination, the material used is *Cyanoacrylate Ethyl* glue and coated with epoxy resin. For coating the stator using epoxy resin it consumes about 24 hours. The wrapped stator is glued to the motor chassis (silver colored) as shown in Figure 4 using contact adhesive glue. This glue material was chosen because it has strong adhesive properties but is elastic enough to dampen the vibration of the motor on the stator. In addition, it is very easy to remove the stator by heating the glue to a certain temperature. The rotor is then mounted on the stator using 13 × 5 mm and 11 × 5 mm bearings. Finally, the shaft locking pin is installed so that the shaft remains in place.

FIGURE 4. Prototyping process of the stator

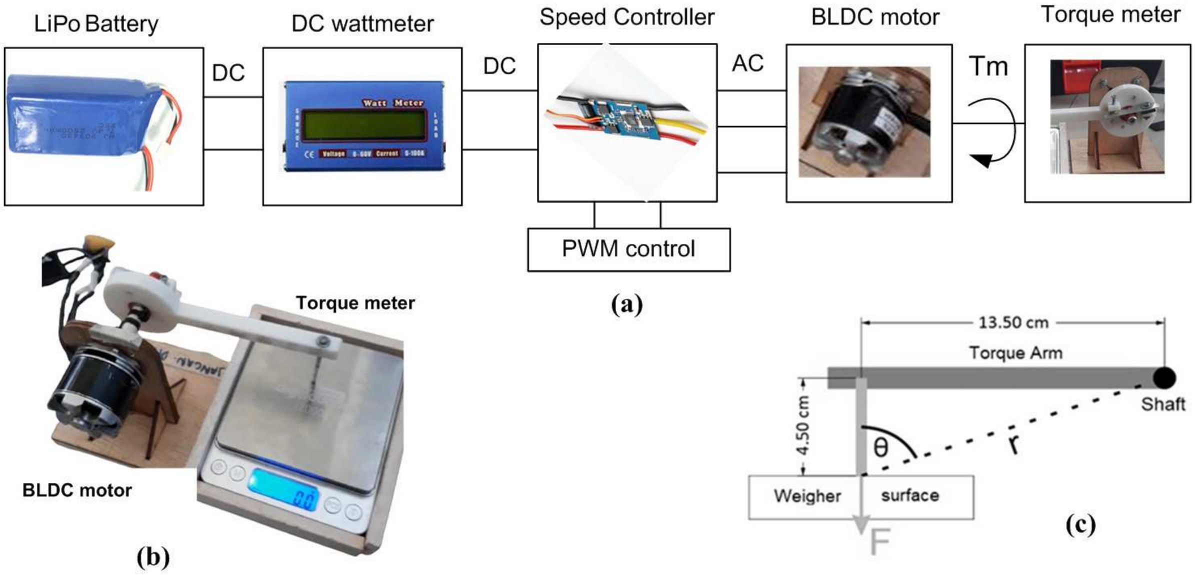

FIGURE 5. (a) Schematic BLDC test; (b) BLDC motor under load torque test; (c) torque arm calculation

3.5. **Testing equipment.** In this study, testing of a three-phase sensorless brushless DC motor prototype was carried out using a four cells (16.8 V) lithium polymer (LiPo) battery as a voltage source, an electronic speed controller, torque meter and its supporting equipment as a regulator of the incoming current to the motor, the tested motor and several measurement equipment. BLDC motor for UAV has a small size so it cannot be measured using a test bench motor that is generally available in the Indonesian market. Therefore, it is necessary to design a special torque meter for BLDC motors for UAVs. The torque meter concept utilizes braking to obtain friction torque. Motor shaft is coupled with the coupling shaft using a locking system. Step for testing the prototype is by connecting 4 cells LiPo battery to the ESC, and gradually the PWM signal from transmitter is increased in order to change the speed of BLDC motor. Then the torque of the BLDC motor is measured by torque meter device as shown in Figure 5(a). Meanwhile, torque meter design can be explained in Figure 5(b). From Figure 5(c), the rated torque of the BLDC motor can be determined by Equation (9).

$$\tau = rF\sin\theta$$
$$\tau = \sqrt{0.045^2 + 0.135^2} \times F \times \frac{0.135}{\sqrt{0.045^2 + 0.135^2}}$$

$$\tau = 0.135 \times F \text{ N·m} \tag{9}$$

4. **Result and Analysis.** In order to know the performance of BLDC motor, here the source voltage is from a LiPo 4 cell with the capacity as 3300 mAh. The test was carried out in stages starting from measuring the speed using the DT-2234C tachometer. The test is limited to a maximum current of 24.78 A or when the torque meter vibrates and does not display the value properly. Before testing the prototype, all dimension of the BLDC motor is measured and compared with the reference motor.

In Figure 6, increasing in current is accompanied by an increase in the input power. When the no-load test, the current should not experience a significant increase. However, because the conductor resistance is 253.7% higher than the standard American Wire Gauge (AWG 32) the copper loss increases exponentially. The maximum copper loss can be proved by the following equation:

$$P_{cu} = 2R_{ph}I_s^2 \tag{10}$$

where R_{θ_A}, R_{θ_B}, R_{θ_C} are internal resistance phases A, B and C, respectively with a delta connection. If only two phases carry current at the same time, copper loss becomes

$$P_{cu} = \left(\left(\left(R_{\theta_A} + R_{\theta_B}\right)//R_{\theta_C}\right) + \left(R_{\theta_A}//\left(R_{\theta_B} + R_{\theta_C}\right)\right)\right) \cdot I_{rms}^2 \tag{11}$$

In this case, if rated current is 14.31 A each phase, then the copper losses become

$$P_{cu} = 1.204 \times 14.312^2$$
$$P_{cu} = 245.55 \text{ W} \tag{12}$$

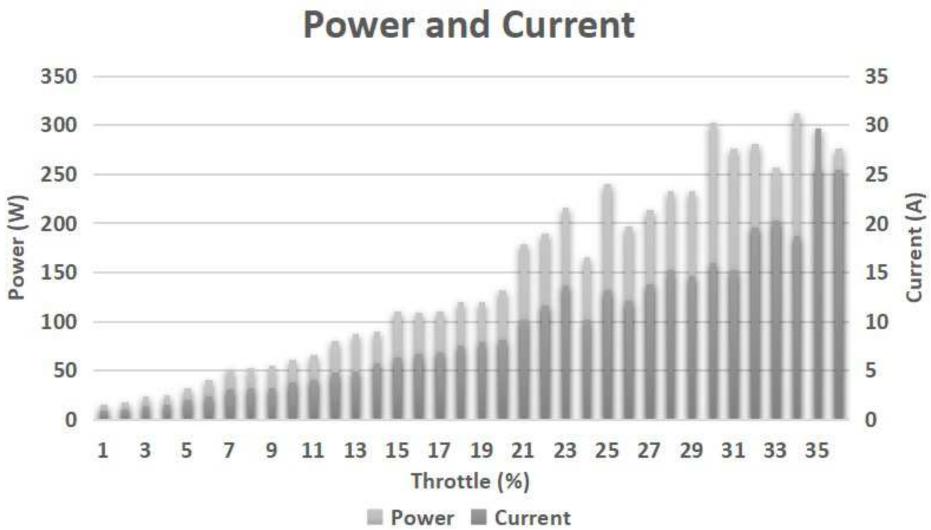

Figure 6. Input power and current

Figures 7 shows the results of the loaded test. In this test the prototype motor is compared with the reference motor AT3520 motor using the same torque meter. It shows that the prototype and reference motor AT3520 have the same characteristics of torque proportional with the speed. While the performance of the prototype motor produces a smaller speed compared to the AT3520 at the same throttle. Figure 8 shows the efficiency of the prototype BLDC motor. It can be explained that, reducing efficiency of the prototype motor is due to many losses inside the motor because of eddy current and copper losses. The available material in Indonesia do not have high efficiency. Therefore, for the next research it is very important to develop material for the machines.

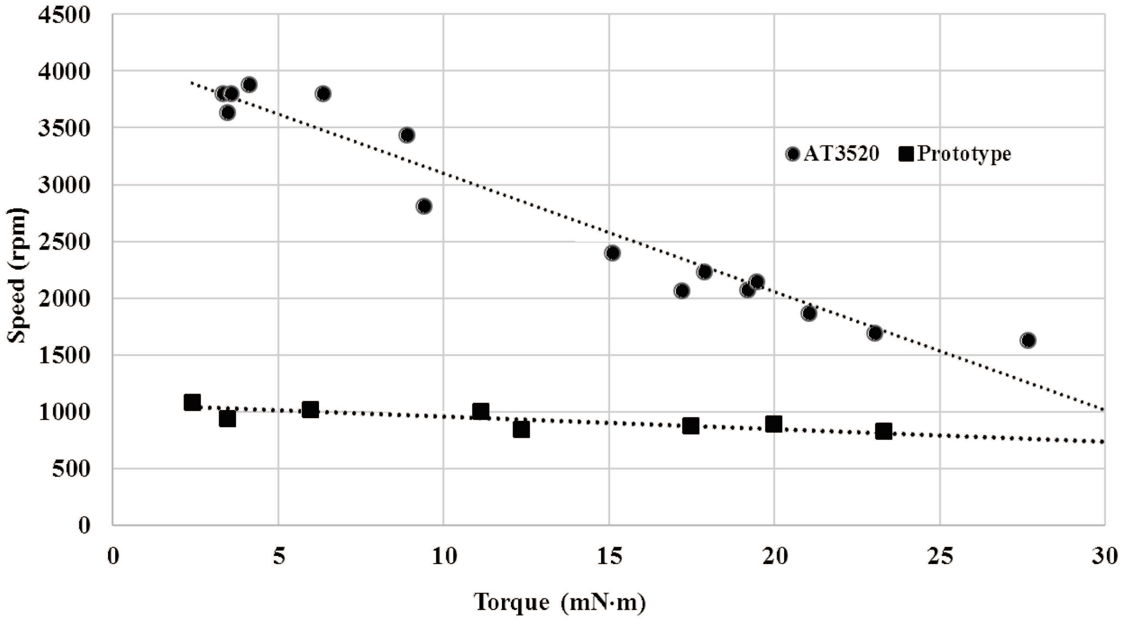

FIGURE 7. Torque vs speed of prototype motor compared with reference BLDC motor

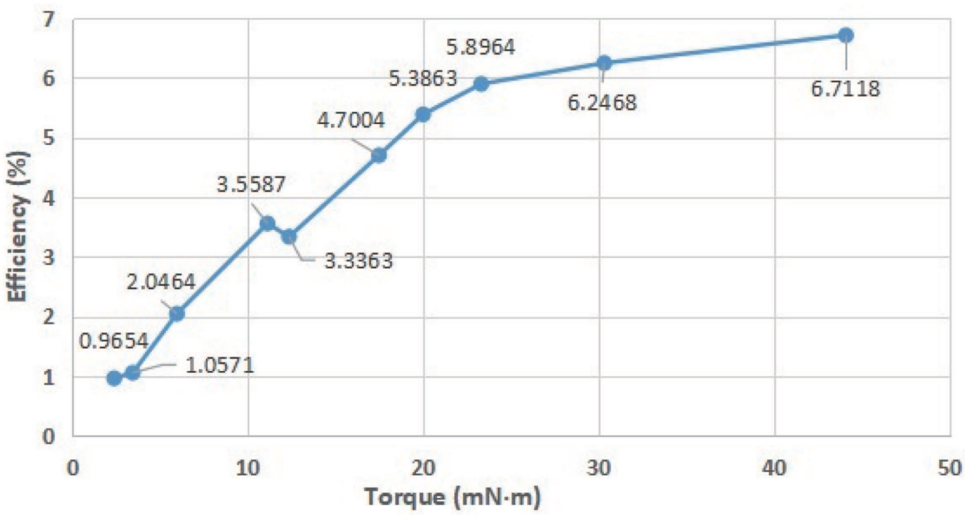

FIGURE 8. Efficiency of the prototype of BLDC motor

5. **Conclusion.** Prototype of BLDC motor for UAV application has been designed and evaluated. It is observed that prototype can work effectively to respond the input command from the signal controlled from the transmitter. The prototype has rated capacity of 811.94 W or 62.45% from original design rated power. Available conductor used in this prototype has resistance 1.37 Ω/m, 253.7% higher than AWG 32 standard of 0.2 mm diameter of wire. Therefore, total copper loss for the prototype is about 246.55 W. Relative efficiency of prototype was measured and calculated 13.57% from original motor. In order to increase performance of the prototype, the next research will consider for selecting and developing high efficiency sheet steel specialized for this BLDC motor. The target is obtaining prototype with high performance with lower budget cost.

REFERENCES

[1] H. Suryoatmojo, M. F. Afif, V. Lystianingrum, E. Setijadi and R. Mardiyanto, Optimal sizing of solar powered unmanned aerial vehicle system for continuous flight based on multi objective genetic algorithm, *ICIC Express Letters*, vol.14, no.8, pp.741-749, 2020.

[2] H. Suryoatmojo, M. Ridwan, D. C. Riawan, E. Setijadi and R. Mardiyanto, Hybrid particle swarm optimization and recursive least square estimation based ANFIS multioutput for BLDC motor speed controller, *International Journal of Innovative Computing, Information and Control*, vol.15, no.3, pp.939-954, 2019.

[3] Y. A. Apatya, A. Subiantoro and F. Yusivar, Design and prototyping of 3-phase BLDC motor, *International Symposium on Electrical and Computer Engineering*, 2017.

[4] M. S. Elkerdany, I. M. Safwat, A. M. M. Yossef and M. M. Elkhatib, A comparative study on using brushless DC motor six-switch and four-switch inverter for UAV propulsion system, *The 12th International Conference on Electrical Engineering (ICEENG)*, 2020.

[5] J. Zhao and Y. Yu, *Brushless DC Motor Fundamentals Application Note*, https://www.monolithicpower.com/pub/media/document/Brushless_DC_Motor_Fundamentals.pdf, 2011.

[6] O. Solomon and P. Famouri, *Dynamic Performance of a Permanent Magnet Brushless DC Motor for UAV Electric Propulsion System*, West Virginia University, Morgantown, 2006.

[7] D. D. Hanselman, *Brushless Permanent Magnet Motor Design*, Magna Physics Publishing, 2006.

[8] S. J. Chapman, *Electric Machinery Fundamentals*, McGraw-Hill, 2005.

[9] P. Yedamale, *Brushless DC (BLDC) Motor Fundamentals*, Microchip Technology Inc., 2003.

[10] J. Kuria and P. Hwang, Modeling power losses in electric vehicle BLDC motor, *Journal of Energy Technology and Policy*, vol.1, no.4, pp.8-17, 2011.

[11] V. Raja, *Introduction to Reverse Engineering*, Master Thesis, University of Warwick, 2007.

[12] D. P. Raymer, Thrust-to-weight ratio and wing loading, in *Aircraft Design: A Conceptual Approach*, Washington, D.C., American Institute of Aeronautics and Astronautica, 1992.

[13] C. Carunaiselvane and S. Jeevananthan, Generalized procedure for BLDC motor design and substantiation in MagNet 7.1.1 software, *International Conference on Computing, Electronics and Electrical Technologies (ICCEET)*, pp.18-25, DOI: 10.1109/ICCEET.2012.6203783, 2012.

[14] H. Suryoatmojo, D. R. Pratomo, Soedibyo, M. Ridwan, D. C. Riawan, E. Setijadi and R. Mardiyanto, Robust speed control of brushless DC motor based on adaptive neuro fuzzy inference system for electric motorcycle application, *International Journal of Innovative Computing, Information and Control*, vol.16, no.2, pp.415-428, 2020.